Pure Appl. Chem., Vol. 76, No. 1, pp. 97–104, 2004.

Ultrasonically induced birefringence in polymer solutions*

Hiroyasu Nomura[1,‡], Tatsuro Matsuoka[2], and Shinobu Koda[2]

[1]Department of Natural Science, College of Science and Engineering, Tokyo Denki University, Hatoyama Hiki-Gun Saitama, 350-0394, Japan; [2]Department of Molecular Design and Engineering, Graduate School of Engineering, Nagoya University, Furo-cho, Chikusa-ku, Nagoya, 464-8603, Japan

Abstract: For ultrasonically induced birefringence in polymer solutions, both the linear sinusoidal birefringence and the nonlinear stationary birefringence were observed. The sign and value of the stationary ultrasonically induced birefringence depended on the molecular structure of segment and its anisotropy in polarizability. Furthermore, no molecular weight dependence could be observed above the molecular weight 10^4. The theory based on the viscoelastic ones using the Rouse–Zimm model could not explain our experimental results as a whole. These results strongly suggest that the stationary ultrasonically induced birefringence should be caused by the local segmental motion of polymer chain in solution. For all polymer solutions investigated here, the stationary birefringence per ultrasonic intensity decreased with increasing frequency. This frequency dependence is not consistent with the present treatment for the ultrasonically induced birefringence.

INTRODUCTION

Ultrasonically induced birefringence has been observed in various liquids and colloidal and polymer solutions [1–15]. For the small anisotropic molecules such as liquid crystals, the orientational relaxation time is smaller or of the same order of magnitude so that the velocity gradient caused by ultrasound can directly induce the sinusoidal orientation. This causes the sinusoidal birefringence, and it is proportional to the ultrasonic amplitude A, that is, the square root of the ultrasonic intensity $\sqrt{W_U}$, since the velocity gradient is proportional to A [1–7,12]. On the other hand, for large anisotropic particles such as colloidal particles, the orientational relaxation time is much larger than the period of the ultrasonic wave so that the orientational motion cannot follow the sinusoidal velocity gradient. However, the radiation pressure, which is one of the typical quadratic acoustic effects, produces the stationary torque on the particle that induces the uniform and stationary orientation of the particles in the solutions [1,8–11]. In this case, the stationary birefringence is induced. The induced birefringence is proportional to the square of the ultrasonic amplitude A^2, that is, the ultrasonic intensity W_U.

From the point of view of detection technique, the both "nonbiased" [1–7,12,13] and "biased" [8–11,13–15] techniques have been used in the experiment of the ultrasonically induced birefringence. The latter can detect only the stationary birefringence since the sinusoidal birefringence is averaged out in the temporal and spatial manner. The former detects the phase retardation by the root mean-square way so that it can detect both the sinusoidal and stationary birefringence. It is very important to use the

*Lecture presented at the European Molecular Liquids Group (EMLG) Annual Meeting on the Physical Chemistry of Liquids: Novel Approaches to the Structure, Dynamics of Liquids: Experiments, Theories, and Simulation, Rhodes, Greece, 7–15 September 2002. Other presentations are published in this issue, pp. 1–261.

‡Corresponding author

nonbiased and biased measurements at the same time to discuss the mechanism of the ultrasonically induced birefringence in polymer solutions.

ULTRASONIC INTENSITY DEPENDENCE OF BIREFRINGENCE IN POLYMER SOLUTIONS

The mechanism of the ultrasonic induced birefringence in polymer solutions is of strong interest since a polymer molecule is a long chain consisting of the small monomer unit.

Recently, we observed not only the root mean square of the birefringence Δn_{rms} by the "nonbiased" technique, but also the stationary birefringence Δn_{st} by "biased" technique in polystyrene (PS)-toluene solutions [13]. Results are shown in Fig. 1 in double logarithmic scale. As is seen in the figure, the birefringence observed by nonbiased detection is proportional to the square root of the ultrasonic intensity, $\sqrt{W_U}$, but that obtained by the biased detection is proportional to the ultrasonic intensity itself, that is, W_U. The values of the birefringence signal measured by the biased detection are smaller than those obtained by the nonbiased detection at all ultrasonic intensities.

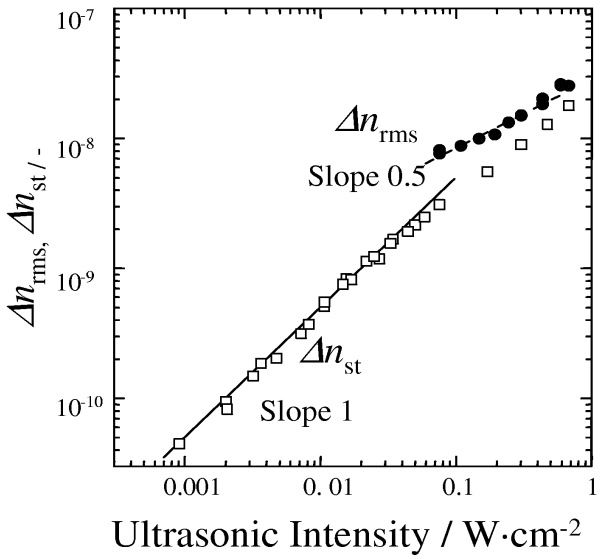

Fig. 1 Ultrasonic intensity dependence of the root mean-square birefringence Δn_{rms} and the stationary birefringence Δn_{st} in toluene solution of polystyrene (10 wt%, 25 MHz, 25 °C) [13]. The solid and dashed lines indicate the slopes of 1 and 0.5, respectively.

Jerrard observed the root mean square of the ultrasonically induced birefringence, Δn_{rms} in PS-toluene and polyisobutylene-cyclohexane solutions using the "nonbiased" technique and found that it was proportional to the square root of the ultrasonic intensity, $\sqrt{W_U}$ [1]. Our experimental results obtained by nonbiased detection were in agreement with those obtained by Jerrard [13]. Moreover, in our measurement by the biased detection technique, the Δn_{st} that was proportional to the ultrasonic intensity was observed in the range from 0.001 to 0.1 W·cm^{-2}. This type of birefringence in polymer solutions has never previously been reported, and our work is the first study.

We derived the expression for Δn_{rms} and Δn_{st} in the polymer solutions based on the stress-optical rule and the Lodge equation as follows [16],

$$\Delta n_{rms} = C\sqrt{W_U / \left(\rho c_0{}^3\right)} \cdot \sqrt{G'(\omega)^2 + G''(\omega)^2} \tag{1}$$

$$\Delta n_{st} = C\left[W_U \Big/ \left(\rho c_0{}^3\right)\right] \cdot G'(\omega) \tag{2}$$

where C is the stress optical coefficient, ρ is the density, c_0 is the sound velocity, and $G'(\omega)$ and $G''(\omega)$ are the storage and loss modulus, respectively.

In order to discuss in more details, the polymer chain dynamics, we will use the Rouse–Zimm theory. The storage and loss modulus are respectively written as,

$$G'(\omega) = (cRT/M)\sum_{p=1}^{P_{max}}\left[\left(\omega\tau_p\right)^2 \Big/ \left\{1+\left(\omega\tau_p\right)^2\right\}\right] \quad G''(\omega) = (cRT/M)\sum_{p=1}^{P_{max}}\left[\omega\tau_p \Big/ \left\{1+\left(\omega\tau_p\right)^2\right\}\right] \tag{3}$$

where $M = N_p m$, m is the molecular weight of the monomer, N_p is the degree of polymerization, c is the mass of the polymer per unit volume, P_{max} is the maximum mode number, R is the gas constant, and T is the temperature. The relaxation time the p^{th} mode is written in terms of the longest relaxation time τ_1 and the scaling constant related to the dimension of the polymer chain ν as,

$$\tau_p = \tau_1 / p^{3\nu} \quad \tau_1 = [\eta] K_1 M \eta_s / (RT) \tag{4}$$

η_s is the solvent viscosity, $[\eta]$ is the intrinsic viscosity, and K_1 is first-order relaxation time factor determined by theory [17]. We compared our experimental results with our expression mentioned above [14]. The results are listed in Table 1.

Table 1 Comparison of the calculation with experiment for the ultrasonically induced birefringence for PS-toluene solutions [14].

	$\Delta n_{rms} \cdot \sqrt{W_U}^{-1}$/cm·W$^{-0.5}$	$\Delta n_{st} \cdot W_U{}^{-1}$/cm^2·W^{-1}
Experiment	3.0×10^{-8}	4.8×10^{-8}
Calculation	1.5×10^{-8}	6.6×10^{-13}

The calculated value of Δn_{rms}, which was proportional to $\sqrt{W_U}$, was in the same order of magnitude as the experimental one. However, the calculated result for Δn_{st} was about 10^5 times smaller than that obtained by the experiments. In our expression, Δn_{st} resulted from the quadratic term in the Finger strain tensor in the Lodge equation. In the framework of the Lodge equation, the nonlinearity is a result of *frame invariance* and the stress–strain relation itself belongs to the linear region [18]. To estimate the Δn_{st} more correctly, nonlinear terms of viscoelasticity and acoustic field should be taken into account.

In order to elucidate the detailed mechanisms of ultrasonically induced birefringence in polymer solutions, it is very important to know the interactions between the segments in a chain. For this reason, it is better to measure the birefringence in lower concentration ranges.

In our study, we focused on the experimental studies about the stationary birefringence because the sign of the birefringence is obtained and the high signal-to-noise ratio is realized [13]. We have started the systematic measurement of ultrasonically induced birefringence in polymer solutions for the molecular structure of segment, concentration, molecular weight, and frequency dependence, and so on [14,15].

MOLECULAR STRUCTURE, CONCENTRATION, AND MOLECULAR WEIGHT DEPENDENCE OF STATIONARY ULTRASONICALLY INDUCED BIREFRINGENCE IN POLYMER SOLUTIONS

Figure 2 shows typical traces of the transient signal of ultrasonically induced birefringence of PS-toluene, polycarbonate (PC)-chloroform, and polybutadiene (PBD)-toluene solutions. The sign of the birefringence was positive for PS-toluene and negative for the PC-chloroform and PBD-toluene so-

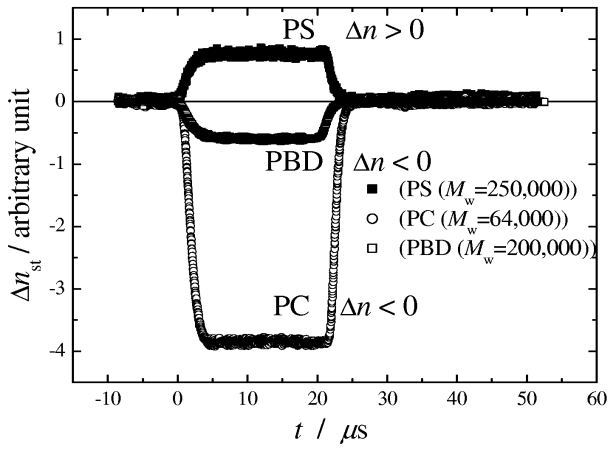

Fig. 2 Traces of the birefringence signal for PS-toluene, PC-chloroform, and PBD-toluene solutions.

lutions. The rise and decay time of the trace of the signal reflects the orientational relaxation times of molecular motions. The rise time of the trace of the birefringence was about 4 μs, which was almost the same as the rise time of the ultrasonic pulse. This means that the orientational relaxation time contributing to the birefringence is smaller than 4 μs.

The difference in sign of birefringence is reflected by the local configuration of polymer chain in the ultrasonic field. It is reasonable to consider that for the flexible polymer chain, the orientation of the segment units of a main chain of the polymer will be perpendicular to the sound propagation. The configuration of the phenyl group will be essentially related to the sign of the birefringence signal. The difference in sign reflects the difference in the way of bonding of the phenyl ring to the main chain structure, as shown schematically in Fig. 3.

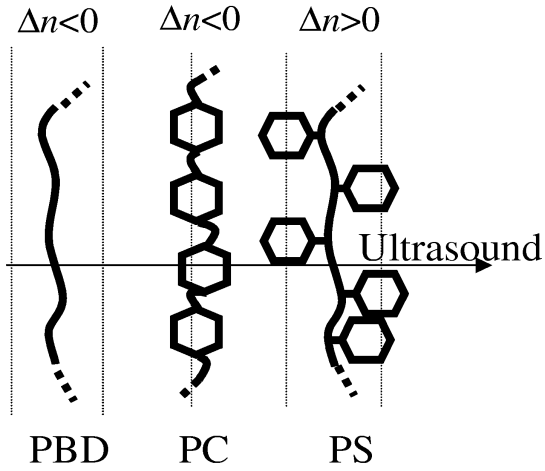

Fig. 3 Schematic illustration of the local orientation of PS, PC, and PBD under the ultrasound.

The concentration dependence of the birefringence per ultrasonic intensity of the PS-toluene, PC-chloroform, and PBD-toluene were shown in Fig. 4. The concentration is represented by the mole number of the monomer unit in the 1 dm^3 solutions. In all solutions, the birefringence increased with increasing concentration. The molecular weight dependence of the $\Delta n_{st} \cdot W_U^{-1}$ value was shown for

PS-toluene solutions at constant concentration of 1.28 mol·dm^{-3} in Fig. 5. At the molecular weight lower than 1×10^4, the birefringence increased as molecular weight increased. However, molecular weight dependence was not recognized when the molecular weight was higher than 1×10^4.

It is well known that polymer solutions show the relaxation processes in the frequency range of MHz, which have been observed by ultrasonic relaxation [19,20] and dielectric dispersion spectroscopy [19]. These relaxation processes arise from the local segmental motions, and the relaxation time does not depend on the molecular weight of the polymer chain in solutions in the region of molecular weight above 10^3 to 10^4. In PS-toluene solutions, no molecular weight dependence of the ultrasonic relaxation spectra was observed above 1×10^4 [19,20]. This *critical* molecular weight of the ultrasonic relaxation is the same as that of the ultrasonically induced birefringence. This suggests that the Δn_{st} is mainly related to the local orientational segmental motions in polymer solutions.

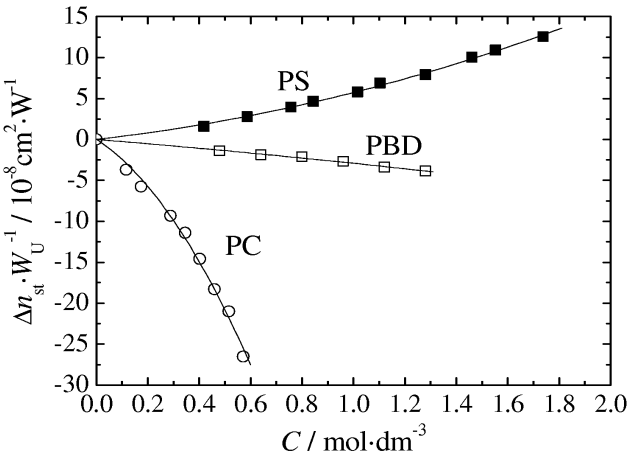

Fig. 4 Concentration dependence of the birefringence per ultrasonic intensity of the PS-toluene, PC-chloroform, and PBD-toluene solutions.

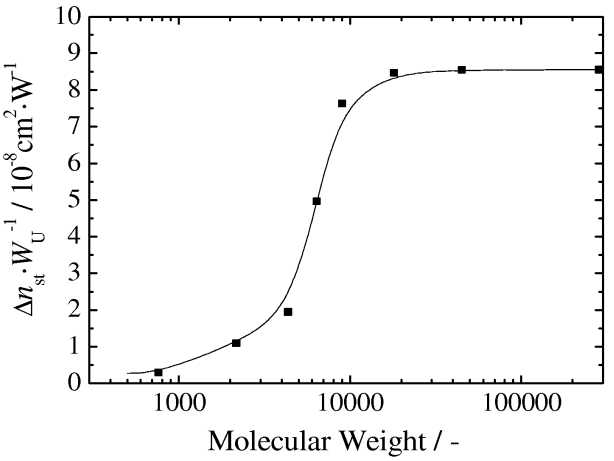

Fig. 5 Molecular weight dependence of $\Delta n_{st} \cdot W_U^{-1}$ for PS-toluene solution at the concentration of 1.28 mol·dm^{-3}.

INTRINSIC VALUES OF THE STATIONARY ULTRASONICALLY INDUCED BIREFRINGENCE AND ITS RELATION TO THE SEGMENTAL ANISOTROPY IN POLARIZABILITY

In order to confirm the local segmental model for Δn_{st} of polymer solutions, we define the intrinsic values of the stationary ultrasonic birefringence and compared to the segmental anisotropy in polarizability, $\Delta\alpha_s$.

Sibce extrapolated values of $\Delta n_{st}\cdot W_U^{-1}/C$ took finite ones, we can define the intrinsic value of Δn_{st} as follows,

$$\left[\Delta n_{st}\cdot W_U^{-1}\right] \equiv \lim_{C\to 0} \Delta n_{st}\cdot W_U^{-1}/C \tag{5}$$

The segmental anisotropy in polarizability, $\Delta\alpha_s$, was estimated from the flow birefringence [21–23]. To compare the birefringence with the anisotropy in polarizability on the basis of the segment unit, the intrinsic values of the birefringence multiplied by the number of monomer unit in a segment, n_s, $[\Delta n_{st}\cdot W_U^{-1}]\cdot n_s$ was calculated. The value of n_s was estimated from the molecular weight of monomer unit, M_0 and the molecular weight of a segment, M_s, which was determined by limiting rigidity of the Rouse mode obtained by the viscoelastic measurements at high frequencies [24,25]. Figure 6 shows the plots the intrinsic values of the stationary birefringence per a segment against the segmental anisotropy in polarizability. The linear relationship is obtained. This means that the stationary ultrasonically induced birefringence of polymer solutions is related to the segmental anisotropy in polarizability of polymer chains.

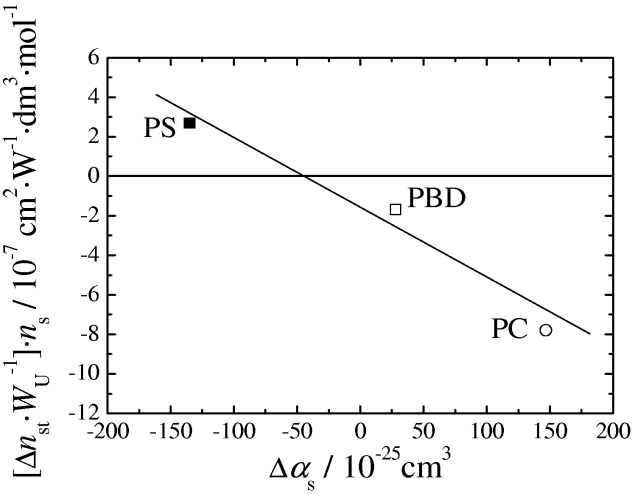

Fig. 6 Plots of the intrinsic value of the stationary ultrasonically induced birefringence per a segment against segmental anisotropy in polarizability.

FREQUENCY DEPENDENCE OF THE STATIONARY BIREFRINGENCE IN POLYMER SOLUTIONS

Frequency dependence of the $\Delta n_{st}\cdot W_U^{-1}$ for PS-toluene solutions is shown in Fig. 7. For all the solutions, the $\Delta n_{st}\cdot W_U^{-1}$ value decreases with increasing frequency in a similar way to "relaxation phenomena" in the frequency range investigated. The difference in $\Delta n_{st}\cdot W_U^{-1}$ values between a lower and higher frequency region increased with increasing the molecular weight. For PC-chloroform and PBD-toluene solutions, the $\Delta n_{st}\cdot W_U^{-1}$ values also decreased with increasing frequency [15].

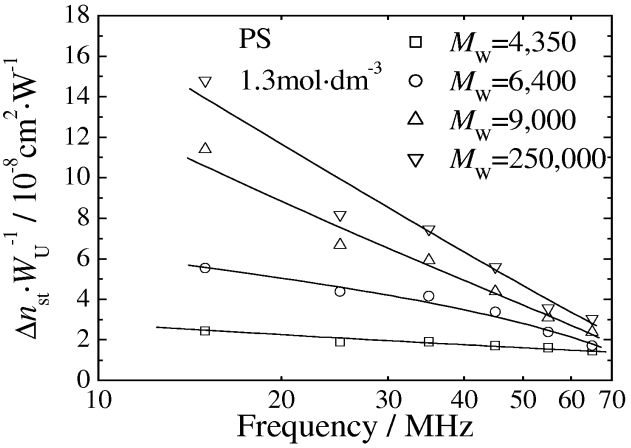

Fig. 7 Frequency dependence of the stationary birefringence per ultrasonic intensity for PS-toluene solutions [15].

For the root mean square of birefringence, Δn_{rms}, in polymer solutions, Jerrard observed that it was proportional to $\sqrt{W_U}$ and the value of $\Delta n_{rms} \cdot \sqrt{W_U^{-1}}$ increased with increasing frequency in the frequency range from 1 to 5 MHz [1]. It can then be concluded that the sinusoidal birefringence, i.e., the linear birefringence, in polymer solutions is caused by the sinusoidal velocity gradient generated by the ultrasound.

For colloidal solutions, the stationary birefringence increased with increasing frequency of the ultrasound [1,8,10]. The radiation pressure caused by the velocity difference between the fluid and the particles produces the torque and it produces the stationary orientation of the disk- or rod-like particle to the preferential direction. The stationary birefringence is then observed. Since the velocity difference between the fluid and particles increases with an increase in frequency in a nonideal fluid, the $\Delta n_{st} \cdot W_U^{-1}$ values increased with frequency.

In polymer solutions, the normal stress difference can be observed and it is well known the normal stress difference is a typical nonlinear effect that comes from the nonlinearity of the Finger strain tensor [18,26]. We put forward a theory of the nonlinear ultrasonically induced birefringence taking into account of the nonlinearity of the Finger strain tensor [16]. However, the estimated value stationary birefringence for the PS-toluene solution 10^5 times was smaller than the experimental value [14]. In addition, the predicted frequency dependence was not consistent with the experimental results in this study.

Frequency dependence of the stationary birefringence in polymer solution observed in this study cannot be explained by the mechanism of for the ultrasonically birefringence discussed so far. Ultrasonic intensity used in the birefringence measurement ranged from 0.001 to 1 W·cm^{-2}. The corresponding pressure amplitude of ultrasound estimated as from 0.054 to 1.7 atm using values of the density and sound velocity of 10^3 kg·m^{-3} and 1500 m·s^{-1}, respectively. Since the pressure amplitude is not so small, the linearization of the fluid dynamics equation is not adequate for our situation. This suggests strongly that quadratic acoustic effect including the streaming will occur in solutions and it causes the birefringence of polymer chains in solutions. Furthermore, in polymer solutions, it is considered that many nonlinear effects, arising from the coupling between local segmental motion and the solvent flow and so on, exist. To clarify the mechanism of the stationary birefringence, the further theoretical treatment including the nonlinearity of fluid dynamics and polymer dynamics should be required.

CONCLUSION

In polymer solutions, the sign and value of the stationary ultrasonically induced birefringence strongly depended on the molecular structure of segment and its anisotropy in polarizability. Furthermore, no molecular weight dependence was observed above the molecular weight 10^4. The theory based on the viscoelastic ones using the Rouse–Zimm model could not explain our experimental results as a whole. These results strongly suggest that the stationary ultrasonically induced birefringence should be caused by the local segmental motion of polymer chain in solution.

For all polymer solutions investigated here, the $\Delta n_{st} \cdot W_U^{-1}$ values decreased with increasing frequency. This frequency dependence is inconsistent with the present theoretical treatment for the ultrasonically induced birefringence, in principle. In order to solve this, it is necessary to measure the ultrasonically induced birefringence with wide ranges of frequency by both biased and nonbiased technique in more details. Also, a new theory is required including the nonlinearity of fluid dynamics and the polymer dynamics for the ultrasonically induced birefringence in polymer solutions.

REFERENCES

1. H. G. Jerrard. *Ultrasonics* **2**, 74 (1964).
2. N. C. Hilyard and H. G. Jerrard. *J. Appl. Phys*. **33**, 3470 (1962).
3. A. Peterlin. *Rec. Trav. Chim*. **69**, 14 (1950).
4. R. Lipeles and D. Kivelson. *J. Chem. Phys*. **72**, 6199 (1980).
5. P. Martinoty and M. Bader. *J. Phys. (Paris)* **42**, 1097 (1981).
6. M. Bader and P. Martinoty. *Mol. Cryst. Liq. Cryst.* **76**, 269 (1981).
7. S. Koda, T. Koyama, Y. Enomoto, H. Nomura. *Jpn. J. Appl. Phys*. **31** Suppl. 31-1, 51 (1992).
8. H. D. Ou-Yang, R. A. MacPhail, D. Kivelson. *Phys. Rev. A* **33**, 611 (1986).
9. K. Yasuda, T. Matsuoka, S. Koda, H. Nomura. *Jpn. J. Appl. Phys*. **33**, 2901 (1994).
10. K. Yasuda, T. Matsuoka, S. Koda, H. Nomura. *J. Phys. Chem*. **100**, 5892 (1996).
11. K. Yasuda, T. Matsuoka, S. Koda, H. Nomura. *J. Phys. Chem. B* **101**, 1138 (1997).
12. T. Matsuoka, K. Yasuda, S. Koda, H. Nomura. *J. Chem. Phys.* **111**, 1580 (1999).
13. T. Matsuoka, S. Koda, H. Nomura. *Jpn. J. Appl. Phys.* **39**, 2902 (2000).
14. H. Nomura, S. Ando, T. Matsuoka, S. Koda. *J. Mol. Liq*. **103–104**, 111 (2003).
15. H. Nomura, S. Ando, T. Matsuoka, S. Koda. *J. Mol. Liq.* In press.
16. H. Nomura, T. Matsuoka, S. Koda. *J. Mol. Liq.* **96–97**, 135 (2002).
17. H. Tanaka, A. Sakanishi, M. Kaneko. *J. Polym. Sci. C* **15**, 317 (1966).
18. R. G. Larson. *Constitutive Equations for Polymer Melts and Solutions*, Butterworths, London (1988).
19. R. T. Bailey, A. M. North, R. A. Pethrick. *Molecular Motion in High Polymers*, Clarendon, Oxford (1981).
20. H. Nomura, S. Kato, Y. Miyahara. *Mem. Fac. Eng. Nagoya Univ*. **27**, 27 (1975).
21. V. N. Tsvetkov. In *Polymer Handbook,* J. Brandrup and E. H. Immergut (Eds.), pp. V-75–V-77, Wiley, New York (1965).
22. J. V. Champion, R. A. Desson, G. H. Meeten. *Polymer* **15**, 301 (1974).
23. J. V. Champion, G. H. Meeten, G. W. Southwell. *Polymer* **17**, 651 (1976).
24. T. Inoue and K. Osaki. *Macromolecules* **29**, 1595 (1996).
25. T. Inoue and K. Osaki. *Macromolecules* **29**, 6240 (1996).
26. R. G. Larson. *The Structure and Rheology of Complex Fluids*, Oxford Univ. Press, New York (1999).